LAWRENCE
LIVERMORE
NATIONAL
LABORATORY

UCRL-CONF-218739

Laser-induced defect reactions governing damage performance in KDP and DKDP crystals

P. DeMange, R. A. Negres, H. B. Radousky, S. G. Demos

February 7, 2006

SPIE Photonics West 2006
San Jose, CA, United States
January 21, 2006 through January 25, 2006

Laser-induced defect reactions governing damage performance in KDP and DKDP crystals

P. DeMange, R. A. Negres, H. B. Radousky, and S. G. Demos

Lawrence Livermore National Laboratory, 7000 East Avenue, Livermore, California 94550

ABSTRACT

The interaction of damage initiating defect precursors in KDP and DKDP crystals with laser pulses is investigated as a function of laser parameters to obtain experimental results that contain information about the type and nature of the defects. Specifically, the focus is to understand a) the interaction of the precursors with sub-damage laser pulses leading to improvement to the damage performance (laser conditioning) and b) the synergetic effects during multi-wavelength irradiation. Our results expose complex behaviors of the defect precursors associated with damage initiation and conditioning at different wavelengths that provide a major step towards revealing the underlying physics.

1. INTRODUCTION

Laser-induced bulk damage sites arising in KDP and DKDP optics used in large-aperture laser systems results in undesirable beam obscuration and downstream intensity modulations, ultimately hindering performance.[1] The damage precursors are believed to be clusters of intrinsic defects and/or nano-particle impurities, however, identifying them has been difficult due to their small size and sparse distribution.[2,3] Laser conditioning provides an increase to the material damage threshold due to an unknown physical process resulting from the interaction of sub-damage laser pulses with DKDP/DKDP defect precursors.[4] In this work, we measure the damage behaviors in DKDP/DKDP pre-exposed to variable excitation parameters to investigate the fundamental mechanisms leading of laser conditioning. We also investigate the damage performance of the pristine material under simultaneous exposure to multiple laser harmonics to probe the relation between damage effects at each frequency of the defect precursor population. The conditioning experiments reveal two distinct pathways leading to conditioning that depend on the pre-exposure fluence and wavelength. The simultaneous damage testing experiments provide the relative absorptivity between each frequency which can be used to predict the performance during frequency conversion.

2. EXPERIMENTAL SETUP

The experimental arrangement has been described in detail elsewhere[5] but the basic setup and approach is described here briefly. The conditioning experiments are performed using a pulsed-Nd:YAG laser. The fundamental (at 1064 nm), second, and third harmonics of the output are separated using high reflectivity mirrors selective to each wavelength. The average fluence of each beam is adjusted using a waveplate and a polarizer. The three beams are then aligned to co-propagate and focused by a 200-mm focal length cylindrical lens to the bulk of the sample. The beams focus to a $1/e^2$ height of 3 mm and widths of 90 μm, 60 μm, and 40 μm for 1064, 532 and 355 nm, respectively. In order to focus each wavelength to the same location in the bulk of the crystal, we have positioned galilean telescopes in each beam line to adjust their divergence before recombination. The beam spatial profiles are measured using a 0.25 by 0.25 $inch^2$ CCD camera with a pixel resolution of ~ 5 μm.

The samples were cut to $1 \times 5 \times 5$ cm^3 size plates and polished on all sides. Bulk damage is produced through the focal range of the cylindrical lens, ~ 8 mm. A counter-propagating 632.8-nm beam from a HeNe laser is focused by a 250-mm focal length cylindrical lens through the back of the sample to illuminate any resulting damage pinpoints in the tested volume. Images of the damaged regions are captured orthogonally to the direction of propagation of the lasers, through the side of the sample. A % 2 magnification microscope objective followed by % 5 magnification lens is used

that provides 4.7 by 4.7 μm^2 per pixel image resolution. Figure 1 shows captured images of scatter from pinpoint damage sites in bulk DKDP that demonstrate both a typical damage measurement and the manifestation of the conditioning effect using this approach. The images capture 5.9 mm in length of the damaged volume along the direction of propagation of the beam. Figure 1a shows damage resulting from a single pulse at 15 J/cm^2 in pristine material and Fig. 1b shows damage resulting from a single pulse at 15 J/cm^2 following pre-exposure to ten pulses at 10 J/cm^2 for conditioning. The damage pinpoint density, or PPD, is measured over the volume exposed to peak laser fluence (± 5%) which is the region enclosed by the white lines shown in each image. Comparison of the two images demonstrates that there is significantly less damage in Fig. 1b (~ 150 pp/mm^3) than in Fig. 1a (~ 1180 pp/mm^3) as a result of having pre-exposed the material to the ten pulses.

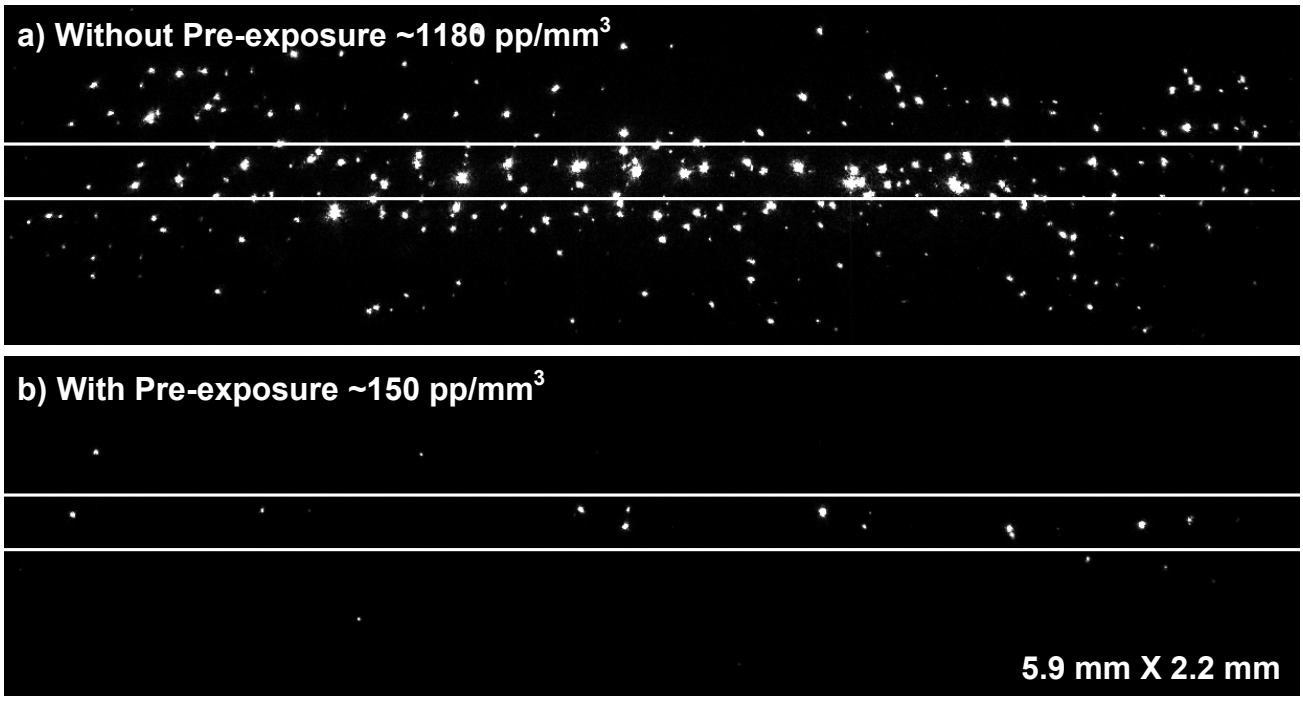

Figure 1. Scatter images of pinpoint damage sites resulting from exposure to a) one pulse at 15 J/cm^2 in pristine material (~ 1180 pp/mm^3) and b) one pulse at 15 J/cm^2 following pre-exposure to ten pulses at 10 J/cm^2 (~ 150 pp/mm^3). The PPD is measured over the volume exposed to peak laser fluence (region enclosed by the white lines).

3. EXPERIMENTS AND RESULTS

3.1. Conditioning vs. Pre-exposure Fluence and Wavelength and Damage Testing Wavelength

The dependence of conditioning on pre-exposure fluence was measured at combinations of damage testing and pre-exposure wavelengths at 1064, 532, and 355 nm. Pristine bulk sites in conventional-growth DKDP were exposed first to ten pulses of the same fluence and then to a single higher fluence damage testing pulse. The fluence of the damage testing pulse remained the same for all sites (46 J/cm^2 for 1064 nm, 31 J/cm^2 for 532 nm, and 23 J/cm^2 for 355 nm) while the fluence of the ten pre-exposure pulses was varied. Images were recorded prior to and after irradiation at a high fluence and the PPD at peak fluence resulting from the damage testing pulse only was plotted versus the peak pre-exposure fluence.

Figures 2a-2c show the density of new damage pinpoints resulting from single-pulse damage testing at 46 J/cm^2 at 1064 nm, 31 J/cm^2 at 532 nm, and 23 J/cm^2 at 355 nm, respectively, as a function of the fluence of the ten pre-exposure

pulses. There are three sets of data in each figure corresponding to pre-exposure at each of the three harmonics. It must be noted that these figures do not include the PPD resulting from pre-exposure.

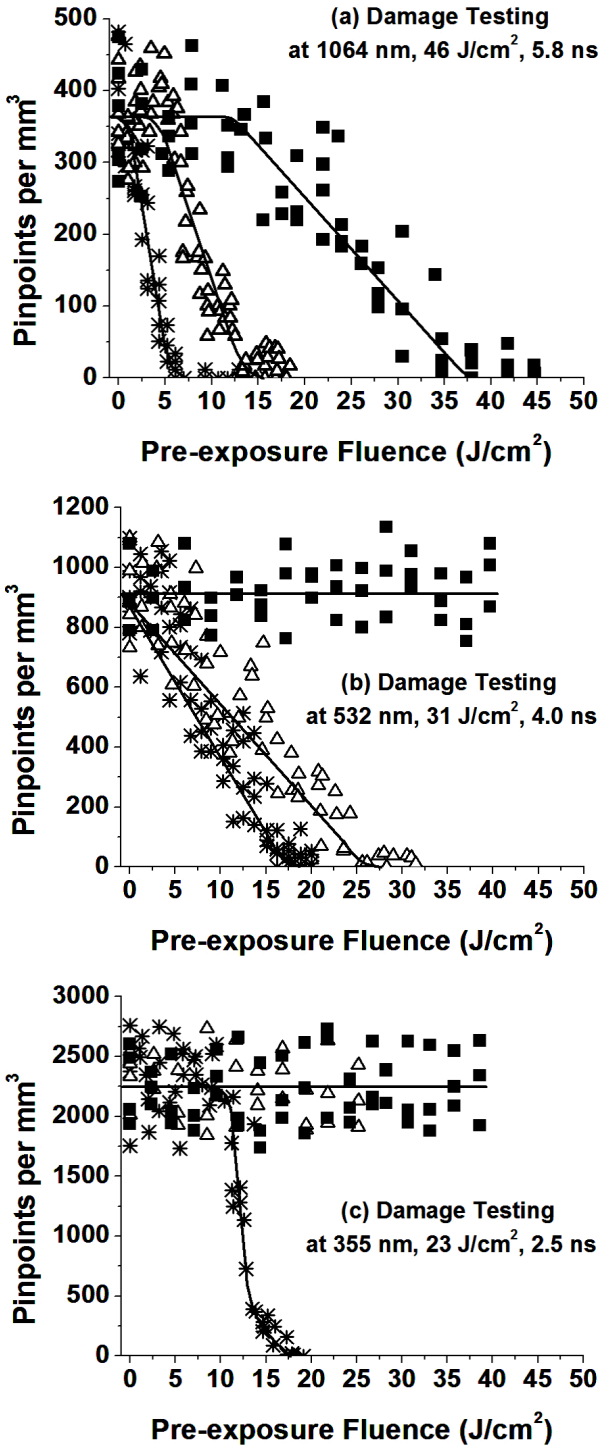

Figure 2. The density of new pinpoints resulting from damage testing pulse at a) 1064 nm at 46 J/cm^2, b) 532 nm at 31 J/cm^2, and c) 355 nm at 23 J/cm^2 as a function of the fluence of the ten pre-exposure pulses (■ = pre-exposed to 1064 nm, < = pre-exposed to 532 nm, and ✳ = pre-exposed to 355 nm) in DKDP.

The density of new pinpoints resulting from damage testing at ~ 46 J/cm^2 at 1064 nm for pre-exposure at each of the three harmonics is shown in Figure 2a. Without pre-exposure, the observed PPD from damage testing is ~ 380 pp/mm^3. Following pre-exposure at 355 nm the results show that the density of new pinpoints after damage testing rapidly decreases with increase in pre-exposure fluence starting from the lowest tested pre-exposure fluence at ~ 0.7 J/cm^2. For preexposure fluence of ~ 6 J/cm^2, the density of new pinpoints decreases to almost ~ 0 pp/mm^3 (from the original ~ 380 pp/mm^3) while the pre-exposure is still below the damage threshold of the material (located at ~ 8 J/cm^2). Pre-exposure at 532 nm shows no conditioning until ~ 6 J/cm^2, demonstrating the presence of a threshold fluence for conditioning. A linear decrease in the density of new pinpoints in then observed with further increase in pre-exposure fluence. Damage testing results in very little or no additional damage for pre-exposure of ~ 14 J/cm^2 and above but this pre-exposure fluence is above the damage threshold of the material (located at ~12 J/cm^2). Pre-exposure at 1064 nm also shows that a threshold pre-exposure fluence exists for conditioning located at ~ 13 J/cm^2 followed by a linear decrease in the PPD. The density of new pinpoints decreases to ~ 0 pp/mm^3 with pre-exposure at ~ 40 J/cm^2, well above the damage threshold at 1064 nm which is at ~24 J/cm^2.

Figure 2b shows the three sets of data for damage testing at ~ 31 J/cm^2 at 532 nm in material pre-exposed at each of the three harmonics. Damage testing without pre-exposure provides ~ 900 pp/mm^3. With pre-exposure at 355 nm, the density of new pinpoints from damage testing appears to decrease linearly with increase in pre-exposure fluence starting from the lowest tested pre-exposure fluence. For pre-exposure above ~ 18 J/cm^2, almost no new pinpoints are observed from damage testing. Similarly, pre-exposure at 532 nm results in a linear decrease in the density of new pinpoints, however, the best conditioning occurs at a much higher pre-exposure fluence of ~ 32 J/cm^2. Damage testing following pre-exposure at 1064 nm up to ~ 40 J/cm^2 indicates no improvement to the damage performance.

Figure 2c shows the three data sets corresponding to the damage testing at ~ 23 J/cm^2 at 355 nm and pre-exposure at each harmonic. Damage testing without pre-exposure provides ~ 2250 pp/mm^3. Similar to the behavior observed for damage testing at 1064 nm and pre-exposure at both 1064 and 532 nm (shown in Fig. 2a), pre-exposure at 355 nm demonstrates the presence of a threshold fluence for conditioning at ~ 10 J/cm^2. However, the density of new pinpoints then rapidly decreases with increasing fluence. Pre-exposure at 532 and 1064 nm up to fluences of ~ 25 J/cm^2 and ~ 38 J/cm^2, respectively, indicate no improvement to the damage performance.

3.2. Damage Testing Under Simultaneous Exposure to 532 and 355 nm Laser Harmonics

The damage behavior of pristine (previously unexposed) bulk material was investigated under exposure to both individual pulses at a single wavelength at incremental fluences and to spatially and temporally overlapping 355- and 532-nm pulses at various fluence combinations. Images were recorded subsequent to irradiation at each of the dual-wavelength fluence combinations and the PPD was measured over the region exposed to peak fluence.

Figure 3 shows the PPD resulting from simultaneous exposure to combination of fluences at 5, 8, 12, 16, 20, and 24 J/cm^2 at 532 nm and 3, 5, 8, 10, 12, 15 and 20 J/cm^2 at 355 nm from one of the tested samples. The data are sorted into sets where the 532-nm fluence is kept constant while the 355-nm fluence is varied. The PPDs resulting from exposure to each wavelength separately are also shown for comparison. In these experiments, the PPD at each combination of fluences was obtained from the average of four tested sites. Similar behaviors were observed in all samples studied although the PPD at a particular fluence combination varied between each material.

The experimental results for this DKDP sample demonstrate that when the 532-nm fluence is held constant at values below 24 J/cm^2, the PPD increases in a nonlinear fashion with increasing 355-nm fluence. However, as the 532-nm fluence is increased above 20 J/cm^2, a transition from nonlinear to a linear increase of the PPD with increase in 355-nm fluence is observed. The results in Fig. 3 also show that the simultaneous dual wavelength exposure results in a much larger PPD than the total PPD resulting from separate exposure at each wavelength. As such, the damage resulting from simultaneous exposure to multiple wavelengths is significant and the damage performance must be considered under conversion conditions.

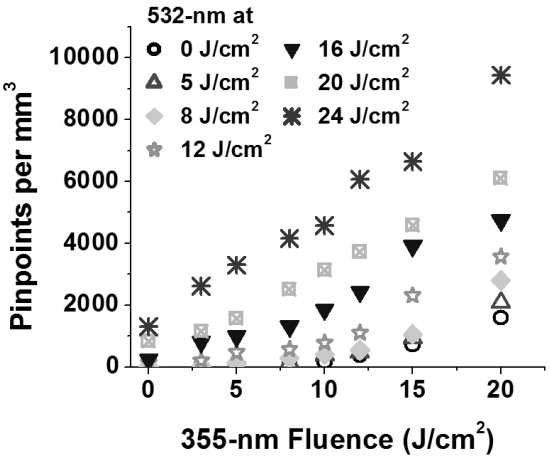

Figure 3. The PPD resulting from simultaneous 532- and 355-nm fluence combinations plotted as PPD profiles at constant 532-nm fluences versus 355-nm fluence.

In order to develop an empirical method to predict the level of damage expected under simultaneous exposure, some basic assumptions regarding the absorption by such defect structures leading to damage initiation at both 532 and 355 nm may be asserted. The energy absorbed at one wavelength may be related to the energy absorbed by another wavelength by a proportionality factor. For example, the fluence absorbed at 355 nm can be related to the fluence absorbed at 532 nm in the following way:

$$\phi_{355} = \gamma(\phi_{532}) \cdot \phi_{532} \qquad (1)$$

This relation assumes the most general possibility in which the proportionality factor $\gamma(\phi_{532})$ that relates fluences at each wavelength depends on the laser fluence (in this case, the fluence at 532 nm).

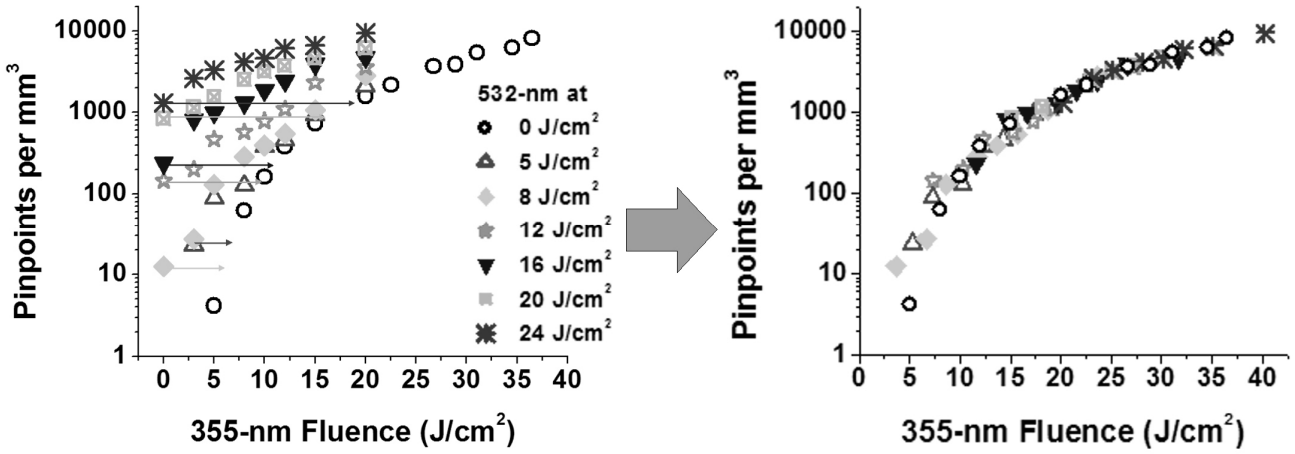

Figure 4. The best fit of PPD profiles at constant fluence at 532 nm (after translation along 355-nm fluence axis) to the 355-nm only PPD profile (shown as **O**).

Applying Eq. (1) to our experimental results is equivalent to translating each PPD profile at constant 532-nm fluence by its corresponding ϕ_{355} along the horizontal 355-nm fluence axis. To realize this approach, we first measured the 355-nm only ($\phi_{532} = 0$) profile over the full PPD range of the data. Next, all of the PPD profiles at constant 532-nm fluence

(shown in Fig. 4) are best fit to the 355-nm only PPD profile. Figure 4 illustrates that each profile overlaps to a section of the 355-nm only profile with a coefficient of determination (R^2) of 0.96 or greater. The results are presented on a semi-log scale to better depict the damage behavior at both high and low PPD values.

4. DISCUSSION

The results of investigating conditioning as a function of the pre-exposure fluence reveal that there are three characteristic damage behaviors. For damage testing at 1064 nm, a "threshold" fluence for conditioning is observed followed by a linear decrease in damage density at higher pre-exposure fluence. For damage testing at 532 nm, a linear behavior is observed with no noticeable threshold fluence. For damage testing at 355 nm, a sharp nonlinear or "step-threshold" behavior is the dominant feature. These different behaviors suggest the presence of either a) different defect populations giving rise to damage at each of the damage testing wavelengths or b) multiple pathways leading to conditioning of the same population of defects.

Figure 4 demonstrates that the PDD (vs 355-nm fluence) profiles at constant 532-nm fluence produced from damage testing under simultaneous 532- and 355-nm irradiation are overlapping to the 355-nm-only PPD profile after translation along the 355-nm fluence axis. This shows that the defects are initiating damage in the same sequence with increasing fluence, independent of the exposure wavelength. This also strongly suggests that the defects leading to damage at 532 nm are the same as those at 355 nm and, moreover, that the absorption mechanisms are the same at both wavelengths. Among this 532- and 355-nm defect precursor population, we have observed two different damage behaviors for damage testing at each wavelength arising from their conditioning. This suggests that there is more than one conditioning pathway in KDP crystals that depends on the laser intensity and wavelength of the conditioning pulses.

The conditioning experiments provide information about the nature with which a specific portion of the defect population is conditioned which is also useful for developing conditioning protocols for operation at each wavelength. For operation at 355 nm in particular, a protocol that uses pre-exposure to 355-nm laser pulses at the conditioning threshold fluence without resulting in damage to the material is desired. The practical implication of the simultaneous 355- and 532-nm damage testing results is that the values of $\gamma(\phi_{532})$ for each profile at constant 532-nm fluence can be extracted using the above fitting procedure to relate the damage effects at one of the wavelengths to those at the other wavelength. This can be used to predict the damage performance during frequency conversion when multiple wavelengths are present.

ACKNOWLEDGEMENTS

This work was performed under the auspices of the U.S. Department of Energy by University of California, Lawrence Livermore National Laboratory under contract W-7405-Eng-48.

REFERENCES

1. J. J. De Yoreo, A. K. Burnham, P. K. Whitman, "Developing KH_2PO_4 and KD_2PO_4 crystals for the world's most powerful laser," *Int. Mater. Rev.* **47**, 113-152 (2002).
2. A. K. Burnham, M. Runkel, M. D. Feit, A.M. Rubenchik, R. L. Floyd, T. A. Land, W. J. Siekhaus, and R. A. Hawley-Fedder, "Laser-induced damage in deuterated potassium dihydrogen phosphate," *Appl. Opt.* **42**, 5483 (2003).
3. C. W. Carr, H. B. Radousky, and S. G. Demos, "The Wavelength Dependence of Laser Induced Damage: Determining the Damage Initiation Mechanisms," *Phys. Rev. Lett.* **91**, 127402 (2003).
4. J. Swain, S. Stokowski, D. Milam, and F. Rainer, "Improving the bulk damage resistance of potassium dihydrogen phosphate crystals by pulsed laser irradiation," *Appl. Phys. Lett.* **40**, 350 (1982).
5. P. DeMange, C. W. Carr, H. B. Radousky, and S. G. Demos, "System for evaluation of laser-induced damage performance of optical materials for large aperture lasers," *Rev. Sci. Instrum.* **75**, 3298 (2004).